CHAPTER 2

CHAPTER 2

LITERATURE REVIEW

The chapter provides a critical review of the published literature on composites and their tribological properties. It begins with a brief description of the composites and their processing techniques, with a special focus on vacuum arc melting, which has been used in the present study. This is followed by a description of tribology, the various types of wear and the parameters that affect the phenomenon of wear, including a brief overview of the fundamentals of friction and some basic friction and wear theories that highlight the many types of wear and Archrad's law [7] (Archard,1953). The chapter also covers the details of the studies conducted for synthesizing the Ti-based composites containing different second-phase reinforcements and evaluation of their mechanical properties. A detailed description of the friction and wear behavior of Ti-TiB composites also forms a part of this chapter. The chapter also presents the gap in the published research, which has helped in the formulation of the problem, and ends with the objectives of the present study.

2.1 COMPOSITE AND ITS TYPES

A composite material is made up of two or more physically and chemically different components. The matrix is the significant and continuous phase, whereas reinforcement is the minor and discontinuous phase. Composites are created to provide desirable qualities for a specific service requirement that a monolithic material cannot offer. The composites were separated into three categories: (i) matrix (metal, polymer, and ceramic), (ii) reinforcing phase (fiber, whiskers, and particle), and (iii) reinforcement geometry (fiber, whiskers,

and particle) (continuous fiber, discontinuous fiber, and wire). Figure 2.1 shows a typical matrix-based composite classification.

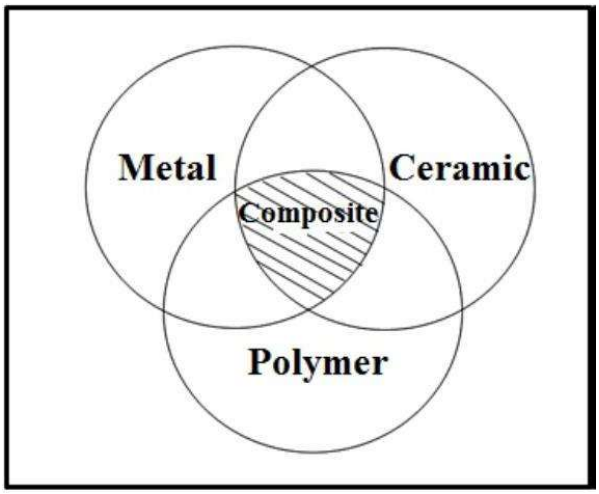

Figure 2.1 Matrix-based classification of Composites. (Rosso et al., 2006)

Metal matrix composites are used in various applications due to their remarkable properties such as high toughness, high specific modulus, high thermal conductivity, and low thermal coefficient expansion. In terms of fire resistance, high-temperature capability, transverse strength, high stiffness, and high shear strength, MMCs outperform polymer matrix composites. Metal matrix composites also have an advantage over ceramic matrix composites in toughness, thermal shock resistance, moisture resistance, thermal and electrical conductivity, and simplicity of workability (joining, shaping, and manufacturing).

2.1.1 DESIGN AND PROCESSING TECHNIQUES FOR COMPOSITES

Metal matrix composites are created using a variety of processing processes. The state of the matrix material mainly determines it at the time of processing. As shown in Fig. 2.2, these processes can be divided into four broad types.

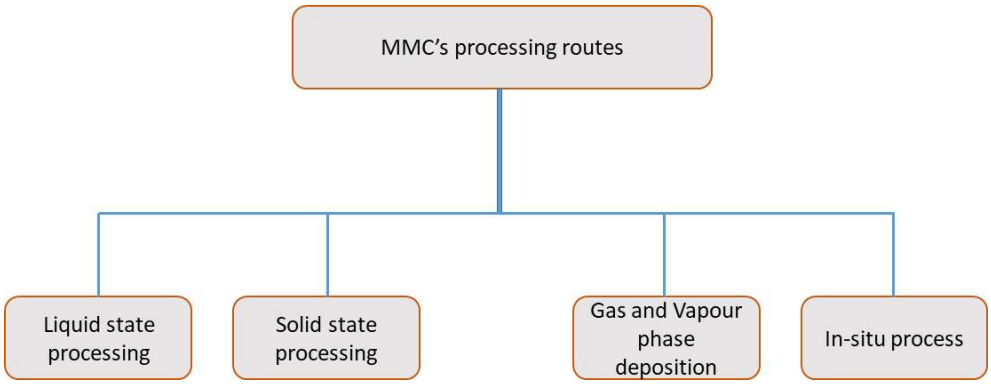

Figure 2 2 Classification of the processing routes to develop MMCs

2.1.1.1 Liquid State Processing

The reinforcing phase particles are introduced into the molten metal during composite preparation in liquid state processing, followed by mixing and casting the melt. Melt stirring, gas pressure infiltration, and squeeze casting are the three types of liquid phase processes that have been identified. The reinforcing phase is added to molten metal and stirred with the help of a stirrer before being allowed to solidify using the melt stirring technique. Although it is a simple composite preparation procedure, high temperatures can compromise the quality of the reinforcement phase. The gas pressure infiltration technique, in which molten metal is infiltrated employing gas pressure to penetrate molten metal into a ceramic, is another liquid phase processing technology. Pore-free casting is an advantage of this technology over other liquid-phase processing methods. **Squeeze casting** is a type of liquid phase processing technology in which molten metal is forced to fill the preform with the help of ram displacement pressure, while the preform is retained at the lower fixed section of the setup.

2.1.1.2 Solid State Processing

Metal is reinforced with particles using a blend of blended elemental powders in this technique. This process involves specific phases before the final consolidation part, and powder metallurgy and diffusion bonding are examples.

(i) Powder Metallurgy (P/M)

It entails combining the matrix and reinforcements in powder form in the proper proportions, compaction under pressure, and sintering at a high temperature to allow diffusion to take place. The procedures for preparing a composite using the P/M technique are shown in Figure 2.3. The approach allows any type or shape of reinforcement, such as whiskers, fibers, or particles, to be used. It's a really versatile approach that allows you to blend materials that can't be combined any other way.

Mixing and Blending: To achieve a homogeneous dispersion of all phases, mixing is done. Elementary powders are mixed, and a homogenous secondary powder combination is produced, with powder particles of proper size and distribution and well-defined morphology. As abrasive, or hard particles, lubricants are added with powders to reduce friction, and wear of compaction dies can abrade the die surface during compaction. This procedure is influenced by a number of factors such as milling time, milling vial and ball material, milling environment, ball-to-powder ratio, processing control agent, and ball size, among others. However, the amount of time spent mixing is crucial. Excessive mixing should be avoided because it can cause particle hardening.

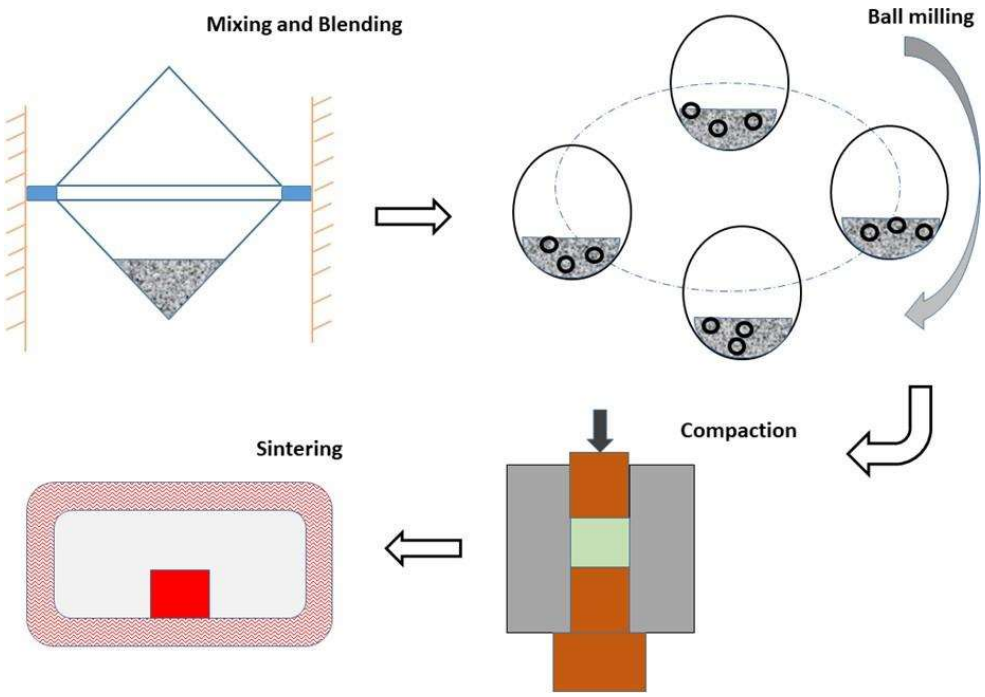

Figure 2 3 Steps involved in the powder Metallurgy process

Due to its efficiency and efficacy in providing a uniform dispersion of small reinforcement phase particles to the matrix phase, high-energy ball milling is the most often utilized mixing method. A planetary ball mill is widely employed in the mixing process because, in addition to mixing, it reduces the size of the powder. It is made out of a jar that is mounted on an eccentric solar wheel both of them revolve in the opposite direction and synchronize the centrifugal force alternately.

Compaction: The technique of compacting mixed powders in a die by applying high pressure at room temperature to generate a green compact is known as compaction. Particle sliding and interlocking, as well as plastic deformation, contribute green strength to compacts. With increasing compaction pressure, compact density rises and porosity falls.

Sintering: Compacts are heated in this method to facilitate the fusing of pores between the interlocking particles, resulting in increased density and strength. It has three stages: in the

first, interparticle welding takes in-between the loosely stacked particles, and the weld expands as the sintering time goes on. The network of pores becomes unstable in the second stage, and it begins to decrease, followed by stage three, in which the pore vanishes. Figure 2.4 depicts the various stages of sintering as well as the diffusion that takes place during the process.

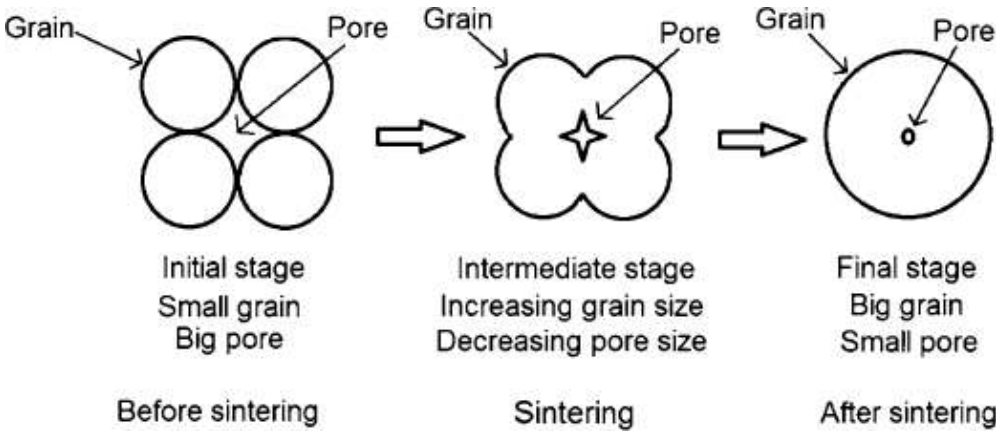

Figure 2 4 A schematic diagram of sintering (Ayatimur et al., 2014)

To create composite materials, many sintering procedures have been used, including traditional sintering, microwave sintering, and spark plasma sintering. Preformed powders are heated for diffusion in the traditional sintering process, which takes place at a temperature below melting point and can last anywhere from a few minutes to many hours. On the other hand, microwave sintering is intimately linked to dielectric characteristics. When a substance is exposed to microwave irradiation, these are recognized as indications. **Hot isostatic pressing** is a sintering technique that involves heating and applying pressure at the same time to achieve high densification. During the consolidation step, joule heating and a simultaneous load are applied in the **spark plasma sintering process**. This sintering happens at a lower temperature than the melting point, and it has various advantages over

conventional sintering procedures, including a shorter sintering time, the avoidance of grain coarsening, and the sintering of phases with a large difference in sintering propensity.

(ii) Diffusion bonding

It's a solid-state technique that involves wrapping metal sheets or foils between fibres to form a sandwich structure. The sandwich of foil and fibre is then compressed and heated to the point at which the foil melts, soaking the fibre and dispersing the metal throughout the structure.

2.1.1.3 Vapor and Gas Phase Deposition

The vapor and gas phase techniques can be categorized generally into two: the vapor deposition processes. and the spray processes

(i) Spray Deposition

A high-speed cold, inert gas (argon or nitrogen) jet is used to break up a crick of molten metal into fine droplets (300 m or less), which are then sprayed along with the reinforcement particulates and collected on a substrate or mould, where the semisolid metal droplets recombine and solidify to create the composite material.[9,10] (Haghshenas et al., 2015; Srivatsan et al., 2006) Droplets flatten down and join together to form the composite shown in Fig. 2.5 when they strike the substrate at a very high velocity in a molten or partially solidified state. Due to the difference in thermal coefficients, even when the splats recombine after the high-energy impact on the substrate, porosity creation is still a possibility. To attain high densification due to the development of various components, a secondary operation like forging is necessary. The spray technique is essentially a hybrid

fast solidification strategy since the metal encounters a quick transition from liquidus to solidus after a delayed cooling from solidus to ambient temperature[11,12] (Campbell et al. 2010; Asthana et al., 2015).

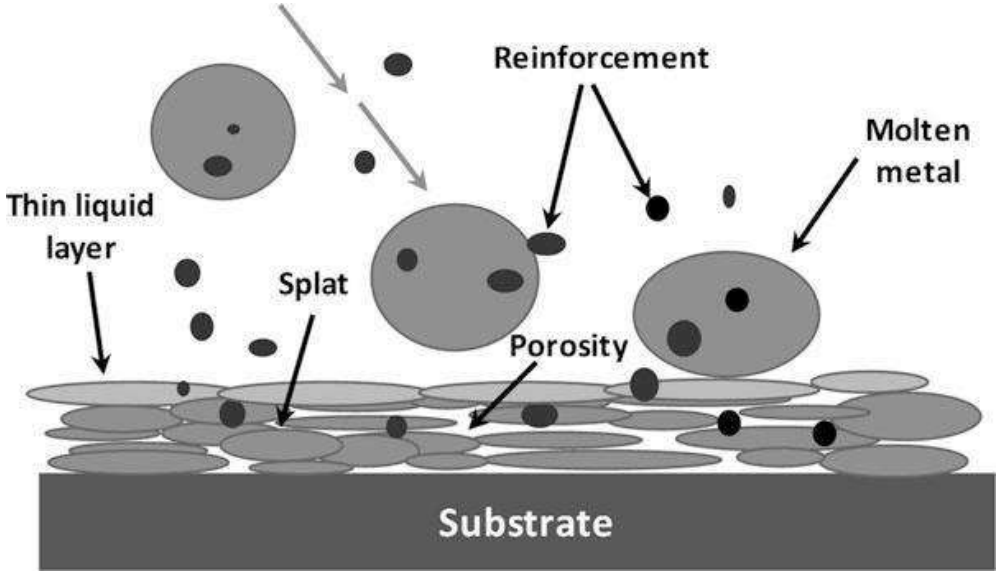

Figure 2 5 Schematic diagram of co-deposition of a metallic matrix and reinforcing particulates via thermal spray process (Asthana et al., 2015).

(ii) Vapor Phase Deposition

Some of the techniques utilised in the process include plasma-assisted chemical vapour deposition (PACVD), physical vapour deposition (PVD), chemical vapour deposition (CVD), and electron beam/physical vapour deposition (EB/PVD) (PACVD). In EB/PVD, fibres are conveyed into the high partial pressure zone of the melt deposit, where condensation takes place, to produce a rather thick coating on the substrate (Shi et al., 2011; Li et al., 2004; Guo et al., 2002)[13-15]. With this technique, a variety of evaporation sources may be used, and the composition can be changed by changing the rate at which the sources evaporate. A wide range of compositions may be prepared, the interfacial area

is not mechanically disrupted, a consistent thickness and thickness control are all benefits of vapour phase deposition. The two primary vapour deposition methods offered on the market are chemical vapour deposition and physical vapour deposition. The process of vaporising solid materials and depositing them on a substrate as a thin film through a chemical reaction is known as chemical vapour deposition. Physical vapour deposition is a vacuum deposition method that involves vaporising a material, then condensing it into a film on the substrate.

2.1.1.4 In-Situ Processing

There are two types of in-situ processes that depend on the regulated solidification of melts (i) uncontrolled solidification of melts (Zhang et al., 2013; Hu et al., 2012; Zhang et al., 2016, Qui et al., 2017)[16-19] and (ii) chemical reaction between two phases (Zhang et al., 2018; lin et al., 2016; Yin et al., 2005; Sui et al. 2014; Peng et al., 2000; Singla et al. 2015)[20-25].

The main benefit of in-situ composite materials is that the reinforcing phase is generally uniformly distributed, and the spacing or size of the reinforcement can be modified in a variety of ways depending on the solidification or reaction time. Because the constituent phase crystallizes in situ rather than being merged from separate sources, the interfaces are clean, mutually compatible, and coherent. However, system selection and reinforcement orientation are limited, and process kinetics (in the case of reactions) or the geometry of reinforcing phases can be difficult to manage at times, as indicated by (Jindal et al., 2019)[26].

2.2 VACUUM ARC MELTING

It is a novel sintering technique, which has been proved to be the most effective one for the research and development of new materials. The liquification → crystallization → 'reversal of the sample → re-melting process is typically repeated to achieve better compositional homogeneity. Arc Melting is used for melting metals typically to form alloys. Materials melted by VAR include high-strength steels, Ni-base alloys, Ti-base alloys, and refractory metals. The triple melt materials are high-qualities materials treated by VIM/ESR/VAR and utilized to manufacture spinning discs for gas turbine engines. Tungsten electrodes create the arc and heat metal powders/particles deposited in a depression (crucible) in the copper hearth. In vacuum arc melting, the chamber is produced vacuum and then refilled with argon gas. As a result, melting occurs in an argon environment. A typical Tungsten Inert Gas (TIG) welding equipment is employed as a power supply. The heat created by the electric arc formed between the electrode and the metals melts the metals in the crucible to form an alloy. Repeated melting is used to increase the alloy's homogeneity. The evacuation of the chamber prevents the melt from oxidizing (Arc being an inert gas does not react with molten metal).

The metals may be heated to temperatures much above 2000^{o}C. Because there are five crucibles in the hearth, a batch of five alloys may be produced in a single evacuation (four small and one large). In the tiny crucibles, around 30g of metal may be melted, and in the bigger crucible, about 100g. The system is comprised of three major components: a power supply (TIG– 600Amp), a chiller, and a vacuum unit. The vacuum unit, which is equipped with rotary and diffusion pumps, can achieve a vacuum of 10^{-6}m bar. The chiller circulates cold water through the copper hearth and electrodes, keeping them cool while they function. After elemental metals (or master alloy) have been melted and hardened, they can be flipped over and re-melted after thoroughly cleaning the furnace. To achieve compositional uniformity, the melting and re-melting procedure is generally done six to seven times.

Aside from the above-mentioned hearth with five crucibles, an extra hearth has been supplied with one crucible, which may suction cast the molten alloy in the shape of thin cylinders (typically 3mm diameter).

2.3 TRIBOLOGY

Relative motion exists between two surfaces in practically every machine component that functions. For reliable performance and effective operation of various machine components, they rely heavily on tribology. The science and technology of interacting bodies in relative motion is known as tribology (Bhushan, 2013)[27]. Friction, wear, and lubrication of surfaces in relative motion under applied force are all covered (Sahoo, 2005)[28]. Friction is a regular occurrence in people's daily lives, as well as in most industrial applications. A machine's efficiency and energy loss can be enhanced, if friction is reduced in some way (Phakatkar, 2009)[29].

The surface wear of material can cause severe damage and failure of the component or machine. (Ludema, 1996)[30]. Friction, we can say, is the mainspring of wear and energy dissipation, and according to Liu et al. (2019), Friction consumes almost half to a third of the energy in the planet. A tremendous percentage of the world's resources are being wasted in some way or another in order to overcome friction. Reinforced metal matrix composites are a good way to reduce friction and regulate wear. Hence, as a result, wear and friction must be decreased or regulated in order for a machine to exist (Bhushan, 2013). A suitable selection of materials, reinforcing, and created microstructure of materials is the most popular method for reducing friction and minimizing wear and catastrophic failure of machine parts or the machine itself.

2.4 WEAR AND TYPES OF WEAR

The wear mechanism is linked to surface interactions, namely the removal and deformation of a material on a fabricated/processed surface as a result of the opposite surface's mechanical action, as Rabinowicz (1995)[33] indicated. Wear is defined as the gradual loss of substance from a body's functioning surface as a result of the rubbing process between two surfaces (Ramesh et al., 1991)[34]. Wear can be classified based on the appearance of worn parts or mechanisms and the conditions that exist during material removal. The types of wear classified according to the wear mechanisms and conditions are: (i) adhesive wear, (ii) abrasive wear, (iii) erosive wear, (iv) impact wear, (v) fatigue wear, (vi) Corrosion and oxidation wear.

Adhesive wear is linked with low sliding velocity, low load, and smooth surfaces are all related with it. This sort of wear can occur in any machine and is difficult to remove; however, it can be mitigated. The asperities interaction on two opposed surfaces in relative motion is the basis of adhesion processes. When the asperities get near together, they may weld, generating a connection at the junction with a rupture strength larger than one of the contacting solid yield strengths. In this situation, a fracture in one of the asperities may occur, resulting in material transfer from one contacting entity to another. **Abrasive wear** develops when two surfaces, one of which is harder and rougher than the other, are in sliding contact. The loss or displacement of material from one surface by the harder asperities of another surface or by harder, loose particles is referred to as abrasive wear. This sort of wear is harmful because it can happen quickly when a contaminant is introduced, resulting in high wear rates. **Erosive wear** is a combination of deformation and cutting that occurs over time. Erosion occurs when the action of fluids and particles gradually wears away a solid surface. Material deterioration can occur under four different

circumstances: (1) solid particle impingement against a solid surface, (2) liquid droplet impingement against a solid surface, (3) flow of hot gases over a solid surface, and (4) cavitation at a solid surface in liquid media. The most important form of erosion is that caused by solid particle impingement. The most common type of erosion is solid particle impingement erosion. **Impact Wear** instead of erosive wear induced by solid particles on a surface, the repeated impact of two surfaces causes impact wear. **Fatigue wear** is described as the cyclically repeated application of a stress state on a component's surface, with each stress pulse causing minor mechanical damage to the surface and subsurface. Finally, the damage builds up to where the surface deforms and/or fractures, failing. Corrosive wear occurs when a chemical reaction at a surface interacts with one or more mechanical wear mechanisms. Sliding surfaces suffer corrosive wear in corrosive environments. On the other hand, the response layer can protect the surface or even act as a lubricant in some instances.

Archard's law defines the inverse relationship between the wear volume loss (W) and hardness (H), which can be expressed as:

$$W = k\frac{L\,S}{H} \tag{2.1}$$

W, k, L, S, and H represent the wear volume loss, wear coefficient, normal load, sliding distance, and hardness of softer materials. (Archard, 1953).

2.4.1 FACTORS AFFECTING WEAR

When two nominally flat surfaces are brought in contact by applying a **normal load**, they only touch each other at the tips of asperities. Hence, the real contact area is much less than the apparent contact area (Archard, 1953). When normal stress brings

together two supposedly flat surfaces, only the tips of asperities come into contact. Due to which the actual contact area is substantially smaller than the perceived contact area. The sum of the areas of all the junctions, which are small regions where the contacting surfaces are close together, makes up the actual area of contact. The apparent area of contact, Aa, is the entire interfacial area, which includes both the genuine area of contact, Ar, and those regions that appear as if contact might have been made there (but wasn't). The number, size, and separation distance of junctions all significantly impact the friction and wear behaviour of sliding contact materials.

According to Rabinowicz (1965), When there is a single asperity contact, the asperity deformation is plastic, and the actual area of contact is directly proportional to normal load, as shown by the equation:

$$A_r = \frac{L}{H} \tag{2.2}$$

Where, L is the average load and H is the initial hardness of the softer of the two materials in contact.

The hardness of the softer of the two materials and the true area of contact given by the contact above equation set the limiting value of the contact interface's pressure, according to Holm (1958) and Bowden and Tabor (1954)[35,36]. They also came to the conclusion that the real area of touch is unaffected by surface topography or the perceived area of contact. As a result, load plays a crucial role in material wear. When the load goes from a lower to a greater amount, the wear rate increases significantly. In general, when the load increases, the friction coefficient increases, and the rate of wear increases, because wear is proportional to frictional force. In terms of burden, there is no discernible pattern. The **contact area** is also important in determining the wear rate of contacting bodies. Wear

is inversely proportional to the contact area. When abrasive particles are exclusively in touch with the surface at a single spot, the friction coefficient is high, and wear increases. The friction coefficient value is lower, and the wear rate is lower when the contact area is more significant. Another important thing to consider is reinforcement, which helps to control wear. The **reinforcement material** has a significant impact on wear. Reinforcement is a strong tool for reducing wear in a variety of moving systems. To offer wear and oxidation resistance, ceramic reinforcements such as TiB, TiB_2, TiC, TiN, and metal oxides (Al_2O_3) are utilized. Reinforcement is nothing more than a way of forming a solid solution, and/or intermetallic could form at the composite material's interface. Because the load must be transferred from matrix to reinforcement through the interface between two mating surfaces, the interface between the metal matrix and reinforcement is critical for the success of composites.

The environment also influences the wear behavior. Environmental factors have a significant impact on material wear. The frictional force is stronger in dry environments, which increases material wear. The qualities of the counter material have a significant impact on the material's wear. When the hardness of the counter surface material is higher than the substrate materials, and the surface quality is poor (work-piece), the wear rate of the counter surface will be lower, and the substrate material will deteriorate faster. The hardness of the abrasive particles in counter material is higher since abrasive particles easily penetrate the substance while operating, causing the substrate material to wear faster.

The **microstructure** is also crucial in regulating how well materials wear. Hardness is lower, and the wear rate is increased when the microstructure is coarse. When the microstructure is fine, the hardness is higher, and the wear rate is lower. The rate of

frictional energy dissipation, and thus the temperature at the sliding interface, is affected by **sliding velocity**. As a result, the sliding velocity has an impact on wear.

2.5 TITANIUM BASED COMPOSITES AND THEIR MECHANICAL PROPERTIES

Several researchers have synthesized titanium-based composites containing different types (hard, soft, or combination) of reinforcements. Various processing techniques to attain desired mechanical properties for a particular service condition and the processing and content of reinforcements have been optimized. The following section presents some research on the preparation and evaluation of mechanical properties of Ti-based composites. With metal matrix composite (MMC), we can obtain attractive properties

Zhou et al. (2022) synthesized Ti6Al4V-5 vol.%TiB composite via selective laser melting (SLM) and reported the microstructure of before and after heat treatment composites show a change in the cluster of TiB whiskers into individual coarsened TiB whiskers with a high aspect ratio resulting in an increase of yield strength by 30% and ultimate compressive strength by 31% of the annealed sample at 950˚C compared to SLM-processed Ti64 alloy.

Wang et al. (2022) synthesized TiB/Ti–6Al–4V composites with a controllable orientation by powder consolidation and hot extrusion via in situ reaction of TiB2 and Ti–6Al–4V and reported an excellent tensile strength due to distribution of the TiB whiskers along extrusion direction without fracture of long TiB whiskers. It has been also reported that controlling the orientation of the TiB whiskers while maintaining the high aspect ratio makes the titanium matrix composite (TMC) exhibit good mechanical properties when the

TiB whiskers are distributed along the tensile axis in comparison to randomly distributed TiB/Ti–6Al–4V composites.

Li et al. (2021) fabricated Ti–6Al–4V alloy (Ti64) and 2 vol.% TiB/Ti–6Al–4V Titanium matrix composite (TMC) via selective laser melting and reported a finer (α+β) dual-phase matrix microstructure for TMC compared to Ti64 above 850ºC. An increased compressive, yield strength and fracture strain were observed due to individually separate TiB whiskers from its precipitate.

Pan et al. (2021) synthesized TiB nano-whiskers reinforced titanium matrix composites (Ti-TiB_w) by selective laser melting (SLM) and spark plasma sintering (SPS) and reported a nano-ultrafine TiB_w reinforced titanium matrix composite with novel nano-reticulated microstructure exhibit exceptional tensile strength of 851 MPa elongation of 10.2%, which effectively improves strength and maintains a reasonable ductility as compared to SPS Ti-TiB_w composites.

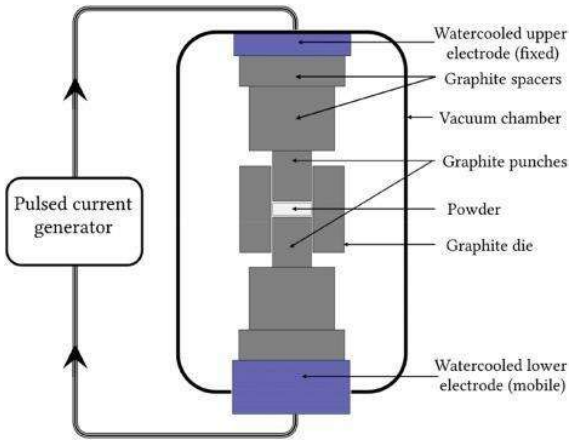

Figure 2 6 Schematic diagram of Spark plasma sintering of powder sample (Guyot et al 2012)

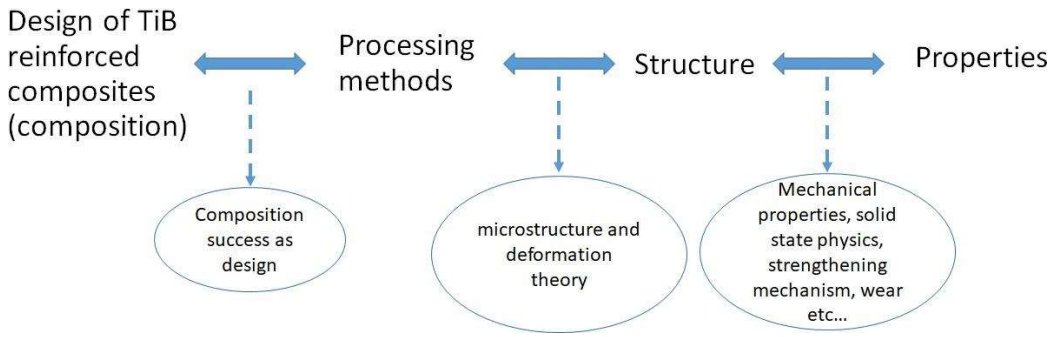

Figure 2 7 Classification of the design and processing routes to develop specific properties in MMCs

Ding et al. (2021) developed (TiB/Ti)-TiAl composites with a laminated structure made by alternating TiB/Ti composite and gamma-TiAl layers by spark plasma sintering and reported the influence of microstructure on mechanical properties of the formed (TiB/Ti)-TiAl laminated composites in comparison to those without laminated have increased fracture toughness and bending strength, also shows good strength and toughness at temperature 150ºC.

Sousa et al. (2021) synthesized in-situ Ti-TiB- TiCx composites by reactive hot pressing and reported an identical corrosion response compared to the unreinforced Ti composites but displayed improved tribo-corrosion behavior. It has been also reported that under 0.5 N load, composites show a 50% less loss in wear volume, also Ti-TiB whiskers don't show any toxicity due to boron due to dissolution and leaching.

In order to analyze the effect of TiB's volume content on Ti-based composites' mechanical properties, the composites have an interconnected architecture of (0, 10, 20, 40, 60, 80, and 100 vol. %) TiB were developed by Ma et al. (2021) in Ti-6.5Al-2.5Sn-9Zr-0.5Mo-0.25Si-1Nb-1W-0.1Er-xB (x = 0, 0.1, 0.2, 0.4, 0.6 and 0.8 wt.%) composite and

reported that 0.2 wt.% boron content is the most appropriate amount for microstructural refinement and mechanical properties enhancement. Aspect ratios of TiB whiskers increase with the increasing boron contents along with strengths increase monotonously, while elongations increase firstly and decrease afterward in alpha-titanium alloys.

Song et al. (2020) fabricated titanium metal matrix composite using 3D ink extrusion printing and sintering and reported a near-full dense high Ti-TiB and Ti-TiC volume fractions up to 25 vol.% in Ti matrix. It has been reported that with the increase in porosity from 24 to 71 %, the compressive strength of Ti-TiB composite drops from 1019 to 55 MPa indicating a high sensitivity of strength with relative density.

Rielli et al. (2020) fabricated in-situ TiB and TiC particles in a β matrix via single-step processing route and reported that increasing the amount of B_4C up to 3% in comparison to other ratios (0,0.5, and 1.5) provided a significant reduction in grain size, compressive yield strength, and ultimate compressive strength with a maximum deformation of 20.5%.

Shafyei et al. (2020) synthesized Ti–TiB–TiB_2 composite via self-propagating high temperature (SPH) and then coated them on Ti6Al4V substrate by Electro-Spark Deposition (ESD) technique under two atmospheres of air and argon, single and double-layer coatings and in two energy levels of 40 W and 110 W and reported that the microstructure shows TiB whisker as main phases along with particle-shape TiB_2 in Ti matrix. It has been reported that the hardness shows an increasing trend with a decrease in energy from 110 W to 40 W.

Liu et al. (2020) used selective laser melting to fabricate lattice structures from TiB_2-Ti powder mixtures of ceramic content (50 wt.% TiB_2), TiB_2 partially transformed into TiB and reported lattice structures of the TiB_2-TiB-TiN composite with ~600 mm pore

diameter maintaining 3.5 MPa compressive strength which increases the viability of TiB_2-TiB-TiN composites, they may be considered as the potential bio-materials.

Zhang et al. (2020) fabricated a continuous gradient Ti/TiB–TiB_2 composite by spark plasma sintering (SPS) combined with tape casting, using 33 tapes of 0 to 80 vol.% of TiB and reported that interfaces between the different thin tape layers were successfully eliminated through the growth of rod-like TiB crystals during SPS sintering. High-speed impact tests of composites with continuous gradient Ti/TiB–TiB_2 having 70 - 80 vol.% TiB show increased anti-penetration performance and can also resist a second strike led to the possibility of a good armor material.

Hirai et al. (2020) fabricated 10 vol.% TiB-reinforced Ti-3Al-2.5V with three different orientation (S, L, and T) and reported the effects of TiB whisker orientation on fatigue properties in Ti-3Al-2.5V by conducting four-point bending fatigue tests for plate-type specimens having three different orientations of TiB whiskers. It has been reported that an increase in fatigue limit and fatigue life of Ti-3Al-2.5V was attributed to TiB whiskers, which are oriented parallel (T) to the loading direction because of the resistances of fatigue crack initiation and propagation.

Zhang et al. (2020) fabricated a series of TiB/Ti composites with different TiB contents by tape casting combined with spark plasma sintering (SPS) to obtain their basic mechanical parameters and reported an increase in acoustic impedance of the TiB/Ti composites moronically with increasing TiB content, but it becomes less effective at high TiB content. It has been reported that the relationship between acoustic impedance and TiB content was divided into three segments according to the linear fitting of acoustic impedance, corresponding to the TiB contents of 5–40 vol.%, 40–70 vol.%, and 70–80 vol.% which attributes in the slopes of the three segments are 0.3226, 0.2031, and 0.0778.

This FGM armor possesses excellent anti-penetration performance and secondary strike ability by optimizing the acoustic impedance matching, as revealed by the ballistic test. The enhanced penetration resistance of FGM armor with a uniform gradient of acoustic impedance than that with a uniform gradient change of TiB content.

Feng et al. (2020) studied the effect of microstructure evolution on the mechanical properties of as-extruded and as-sintered TiB_w/TA15 (nominal composition, Ti-6Al-2Zr-1Mo-1V) and reported that as-extruded composite show an increased, ultimate tensile strength, elongation and vickers hardness when compared with as-sintered composites. It has been reported that there are optimistic application prospects for these TiB_w/TA15 TMCs in aerospace, military, and seafaring.

Hu et al. (2019) fabricated TiB/Ti6Al4V composites and studied the coarsening, and agglomeration of TiB-whiskers in titanium matrix composites during the multi-pass hot deformation process and reported an increase in the aspect ratio of TiB whiskers without change in diameter which results in increased yield strength of the TMC in comparison to the single pass TiB/Ti6Al4V composite.

An et al. (2019) fabricated 50 vol.% (TiB + TiC)/Ti64 composite coatings with different TiB/TiC ratios by gas tungsten arc cladding (GTAC) on the network structured 3.5 vol.% TiBw (TiB whisker)/Ti64 substrate, further ball-on-disc dry sliding wear tests were carried out to assess the abrasion resistance of the samples with a SAE52100 steel ball of diameter 6 mm as counter body, under a load of 9.8 N, a sliding speed of 498 rpm for 0.5 h and reported that primary TiB and TiC exhibited much larger sizes than their eutectic counterparts, and the two-scale reinforcements formed by the dissolution-precipitation mechanism predominated the hybrid coatings which result in an increase in abrasion, low wear rate of coatings in comparison to the substrate.

Huang et al. (2018) prepared TiB_w/Ti6Al4V composite through a gas tungsten arc welding process and reported that the reinforcements in the heat-affected zone (HAZ) remained unaltered, but the reinforcements in the fusion zone (FZ) were refined with refined network size. It has been reported that an increase in the microhardness, yield, and tensile strength compared to Ti6Al4V is due to the TiB phase.

Hu et al. (2018) synthesized in-situ TiB-reinforced titanium matrix (TiB-Ti) composites using four levels of laser power(i.e 125 W, 150 W, 175 W, and 200 W) for the deposition via an additive manufacturing process and reported a three-dimensional quasi-continuous network (3DQCN) microstructure within TiB-Ti composites which resulted in an increase of both strengthening and toughening effects on TiB-Ti composites leading to increase in yield strength and wear resistance with 200 W laser power.

Chandran et al. (2016) synthesized nanostructured TiB in Ti-TiB-Fe-Mo composites by electric field activated reaction sintering(EFAS). The electric power was controlled to provide 100 deg per min heating rate and to reach 1350 deg Celcius and 20 MPa pressure was applied upon reaching the holding temperature. The sample was dense and increased hardness with increasing TiB in composition. The properties were found to be enhanced compared to the commercially available silicon nitride.

Zhang et al. (2015) fabricated a 0-100 vol.% of titanium boride/titanium (TiB/Ti) composites via a hot pressing furnace and reported the phases and microstructure effects on mechanical properties. It has been reported that the microstructure evolution plays an important role during compressive and flexural strength test and result in an increase till 80 vol.% then a decrease for 100 vol.%, Whereas elastic modulus increases with TiB increases in the composition.

Zhang et al. (2015) fabricated six-layered functionally gradient material (FGM) of Ti–TiB–TiB_2 via spark plasma sintering under 40 MPa for 5 min and reported a well-bonded composite structure consist of only TiB and Ti phase. It have been also reported that an increase in hardness was observed from 0% to 50% volume fraction of TiB revealing that TiB phase has two morphologies, i.e. needle shape and agglomerated TiB in the microstructure of the synthesized FGM.

Makau et al. (2013) sintered Ti-TiB composites through SPS and reported the biocompatibility of Ti-TiB_w composites for applications in medical and dental implants along with the attachment of fibroblast with the Ti-TiB composite. It has been also reported that the bio response of these composites shows a better response with blood, and a good growth rate of cells cultured in low hemolysis when compared to pure Ti and Ti-6Al-4V which makes Ti-TiB_w composite suitability as a biomaterial.

Zhang et al. (2013) fabricated four-layer TiB–Ti functionally graded material system using graphite die with and without area-changing cross-section via spark plasma sintering and reported that a fine and dense microstructure with continuous and crack-free interfaces, increased micro-hardness at the layer interfaces, also each layer in the TiB–Ti system functionally graded material has higher bending strength and fracture toughness than the corresponding layer in the material synthesized using the standard cylindrical die.

Liu et al. (2013) prepared a novel laminated Ti–TiB_w/Ti composites composed of Ti layers and TiB whisker reinforced Ti (TiB_w/Ti) composite layers by reaction hot-pressing and reported that in-situ produced TiB whiskers inhibit Ti matrix grain development in the TiB_w/Ti composite layers. Also, tensile testing showed that the laminated composite's maximum strength and ductility were raised to 617 MPa and 20.5 percent, respectively, compared to pure Ti 546 MPa and 17.5 percent.

Kumar et al. (2012) fabricated two volume fractions of Ti-TiB composites via by three powder metallurgy techniques spark plasma sintering, hot isostatic pressing, and vacuum sintering, and reported different morphologies like a needle, short agglomerated, and fine plate. It has been reported that with an increase in volume fraction the hardness, elastic modulus and mechanical characteristics increase but poisson's ratio decreases. Composites processed via SPS and HIP exhibit better overall performance.

Zhang et al. (2012) synthesized 2.5, 5, and 7.5 vol.% (TiB + TiC) volume fractions composites by casting and reported an increase in yield strength and ultimate tensile strength result but ductility decreases significantly. It has been reported that elastic modulus increases with the increase in volume fraction of (TiB + TiC) at room and 650 ºC

Koo et al. (2012) fabricated nanosized TiB whiskers in Ti–6Al–4V via spark plasma sintering and reported a higher aspect ratio of 58 resulting in 3 times more effective strengthening than low aspect ratios. It has also been reported that the high load-bearing capability of TiB whiskers with a diameter of 100 nm produced in situ in a Ti alloy matrix is responsible for the strengthening.

Zhang et al. (2012) fabricated 7.5 vol.% TiB/Ti composite sheet through a casting route followed by 1-D forging followed by multi-step rolling and reported a decrease in aspect ratio and an increase in fracture toughness with an increase in as-cast followed by as-rolled composite compared to as-cast composites.

Huang et al. 2011 fabricated 2, 3.5, and 5 vol.% in situ TiB/Ti6Al4V composites and reported whisker-rich and lean region-like microstructure, which imparts better strengthening and resists the formation of fracture. It has been reported that the lean region of TiB favors the failure of composites during composite elongation in fracture tests.

Kooi et al. (2003) used laser arc cladding to coat Ti-6Al-4V substrate with in-situ Ti-TiB with a Ti/TiB_2 mixed powder and reported 3 different types of microstructure morphology in the basis of shape and size of TiB (a) needle if the diameter is 200 nm and length 15 m, (b) plate if needle if thickness 1 m, short length 3 m, and long length 15 m and (c) coarse needles if diameter 3 m, length 50 m development under fast-growth conditions. It has been also reported that increased fracture toughness and hardness of the composites coating is due to the addition of TiB in Ti matrix and the results predicted a considerable boost in Ti wear resistance.

Li et al. (1993) fabricated Ti-6AI-4V matrix with discontinuous TiB whiskers composites via powder metallurgy followed by hot extrusion and reported ultrafine TiB_w insertion in Ti matrix observed by using high-resolution electron microscopy (HREM). It has been also reported that aspect ratio increases more than 20 after hot extrusion, and interfaces of the TiB/Ti found to be atomically flat, sharp, and free of any interfacial phase.

2.6 DRY SLIDING OF TITANIUM BASED COMPOSITES

Titanium based composites have been studied extensively for its tribological behavior under different loads, sliding speed and composition by many researchers. Some of the studies are presented here:

2.6.1 CONTAINING TiB PHASE IN Ti MATRIX

Wang et al. (2021) synthesized TiB-reinforced Ti-based composite coatings modified with (0,1, and 2 wt.%) Y_2O_3 on Ti-6Al-4V alloys by laser cladding then perform a dry sliding wear test with a rotating abrasive wheel (HRC60) under 49 N load for 60 minutes at 200 rpm. It has been reported that 1% Y_2O_3 enhances the wear resistance of the composite due to the morphological conversion of TiB from needles to plates, which also

results in enhanced load-bearing due to the large-sized TiN and TiB units, ultimately, improving the tribological properties of the coatings.

Kumar et al. (2021) fabricated an in-situ metal-ceramic composite of 50 wt.%Ti–50 wt.% TiB_w by spark plasma sintering further perform ball-on-plate dry sliding wear tests against a 10 mm alumina ball under 5 N normal load at RT and elevated temperatures of 300 ˚C, 500 ˚C, 700 ˚C, 800 ˚C, and 900 ˚C and reported a reduced wear rate of Ti-TiB_w composites in compare to pure Ti due to formation of protective tribo-oxide layers on the surfaces of Ti-TiB_w. The coefficient of friction (CoF) dosen't show any specific trend, the highest load bearing capacity (26 N) in combination with a lower CoF (<0.2) of the generated tribo-oxide layer was demonstrated at 800 ˚C.

Selvakumar et al. (2020) synthesized Ti-TiB based composites containing 20 and 40 vol. % of TiB by three different processing methods vacuum arc melting (VAM) vacuum sintering (VS), hot isostatic pressing (HIP) further dry sliding fretting-reciprocating wear test of titanium boride (TiB) particles against bearing steel balls at 10, load of 5 N, 10 N and 15 N, with a frequency of 50 Hz and 2 mm stroke length and reported that an increase in hardness and indentation fracture using the nano-indentation technique. It has been also reported that the load–depth curves of indents for Ti–TiB shows the deviations of the modulus of elasticity, and composites prepared via SPS show an overall better performance in terms of wear resistance and coefficient of friction in comparison to the other two processing methods, suggest it can be used in the automotive brake pad, precision manufacturing, and locomotives to avoid critical wear failures.

Toptan et al. (2020) produced highly porous Ti, Ti-TiB-TiN_x in-situ hybrid composites by pressureless sintering using BN as a reactant and carried out dry sliding reciprocating wear test against a 10 mm diameter alumina ball under 3 N of normal load, 4

mm stroke length, 1 Hz of frequency and for 30 minutes. It has been reported that in situ reinforcing phases led to an increase in the hardness, as well as an increase in wear resistance also, electrochemical studies in PBS revealed no localized corrosion in porosity or the in-situ phases formed.

Zheng et al. (2020) synthesized in situ (TiC + TiB) of 0, 2, 4, 6, 8, and 10%. volume fractions in titanium matrix composites (TMCs) via melting cast process and carried out dry sliding pin-on-disc wear test with counter body Cr12MoV forged steel (58-60HRC), at100 N for 30 min at a sliding speed of 0.11 m/s. the needle-like morphology of TiB was observed resulting in an increase in hardness and wear resistance. It has been reported that 10% vol. (TiC + TiB) shows the lowest wear among all composites the and wear mechanism was found to be oxidation, abrasion, and adhesion.

Xia et al. (2019) synthesized four in-situ TiB and TiC hybrid strengthened Ti-based composites through laser powder-bed fusion (LPBF) of the B4C/Ti composite powder system with varying laser speed and carried out dry sliding reciprocating wear test was performed on all four composites with GCr15 alloy ball (4mm), stroke was kept 1mm with a normal load of 20N, the frequency was kept at 5Hz for a test duration of 20 min. It has been reported that an increase in porosity with an increase in laser scan speed (i.e 600,1000,1400, and 1800 mm/s) while minimum wear was observed for 1000mm/s with a low average coefficient of friction.

An et al. (2018) investigated the ceramics reinforced titanium matrix composites (TMCs) exhibited high specific strength, especially with special network architecture, and reported that in-situ TiB_w enhances hardness, resists abrasion with the mechanism varied from micro-cutting to brittle debonding with increasing TiB_w content, and increasing network size caused the increase of COF along with wear loss. It has been

also reported that the composite with 8.5 vol.% TiB_w and a network size of 60 μm exhibited the best wear properties. Due to heat treatment, the microstructure transformation into β phase with TiB and subsequent heat treatment further enhanced the abrasion resistance and resulted in a decrease in COF and increased wear resistance.

An et al. (2018) synthesized TiB/Ti64 composite coatings by a two-step method and reported that the thick composite layer reinforced by two-scale TiB is well bonded with the substrate i.e as-sintered 3.5 vol.% TiB_w/Ti64 subjected to ball-on-disc wear test under normal load of 30g and sliding speed of 300rpm against Si_3N_4. ball of dia 6mm. It has been reported that a decrease in the coefficient of friction is observed in comparison to the substrate material and an increase in the hardness, modulus, and wear resistance of the composite is due the coating surface on the substrate.

Hu et al. (2018) fabricated in-situ TiB-TMCs by laser-engineered net shaping (LENS) and reported the formation of a flower-like microstructure at high B content and low B content shows a cross-linking microstructure, and a dry sliding wear test was conducted over a 5m sliding distance with a steel (HRC60) ball bearing counterface under 0.2N of normal load and a constant 3 mm/s sliding speed. It has been also reported that aggregated TiB joins the edge of Ti to form a 3D link network microstructure. When compared to commercially pure Ti bulk components, TiB-TMCs had higher wear performance (i.e. indentation wear resistance and friction wear resistance) due to the presence of TiB reinforcement and the novel microstructures produced inside TiB-TMCs.

Tao et al. (2018) fabricated three TiB whiskers (TiB_w) reinforced titanium matrix composite (TiB-TMCs) by varying the energy input of electron beam remelting, also perform the wear test against the Si_3N_4 sphere having a diameter of Φ12.7 mm, a constant normal load of 10 N with reciprocating frequency of 10 Hz and oscillating

amplitude of 1 mm for 20 min. It has been reported that the quasi-continuous network (QCN) structure along with the dispersive structure in the depth direction of the remelted area having a gradient hardness enhances the wear resistance by tailoring the architecture of TiB_w in TiB-TMCs.

Bao et al. (2018) fabricated 20vol.%TiB/Ti coatings synthesized by inert tungsten gas (TIG) with varying the speed of wire-feed deposition (WF-D) at 5 mm/s and 13 mm/s further performing dry sliding pin-on-disk wear test to assessed the anti-wear performance of the coated pin and uncoated pin (counterpart: tungsten carbide, load: 10 N, sliding speed: 1.5 m. s^{-1}). The coated pin shows an enhanced wear performance compared to the uncoated pin, extending the applications of titanium (Ti) and related alloys in wear settings.

In another study, Chaudhari et al. (2018) studied the tribological behavior of Ti/TiB/TiC hybrid composite processed by spark plasma sintering (SPS for the first time, KBF4 was utilized as a boron precursor, and it interacted with Ti to create the TiB reinforcement in situ and reported that foils made of graphite were a source of carbon for TiC which is observed in both composites and carried out a pin-on-disc wear test at 40 N, speed of 1m/s against hardened steel disc (RC 65) for a distance of 1000 m. It has been also reported that the microstructure obtained of the composite show ultrafine TiC, fine TiB needles on the surface, graded with coarser TiB whisker-reinforced Ti (Ti-4Al-2Fe/TiBw) which leads to enhanced hardness and wear resistance of composite in comparison to the Ti-4Al-2Fe/TiB composite.

Izui et al. (2018) fabricated TiB and TiC-reinforced pure Ti matrix composites by using the spark plasma sintering (SPS) technique. It has been reported that the effect of addition titanium and its alloys have excellent strength properties and corrosion resistance,

but they show poor wear resistance, which cannot be improved by heat treatment. It has been also reported that incorporating hard ceramic particles into a titanium matrix composite is an efficient approach for increasing the wear resistance of titanium and its alloys. TiC and TiB_2 were selected as reinforcement materials because a composite comprising these reinforcements has high tensile strength and a unique microstructure. A ball-on-disk type testing equipment was used to conduct dry sliding wear tests on the composites. The impacts of reinforcement material, microstructural characteristics, and reinforcement volume percentage on composite wear behavior were studied. The specific wear rates of both composites reduced as the reinforcing volume fraction increased. At a reinforcement volume percentage of 25%, the specific wear rate of the TiC/Ti composite decreased dramatically. TiC/Ti composites with reinforcement volume fractions greater than 5% demonstrated superior wear resistance when compared to TiB/Ti composites. The wear behavior of the composite was primarily determined by the distribution of reinforcement material and the type of reaction products formed by the matrix and reinforcement particles.

Attar et al. (2017) synthesized Ti and Ti-TiB composites using selective laser melting (SLM) with a distribution of needle-like TiB particles across an α- Ti matrix and reported that using stresses of 2, 5, and 10 mN, nanoindentation to examine hardness (H) and decreased elastic modulus (Er). It has been also reported that with increased hardening the stiffness increases which show the higher value of H and Er in comparison to Ti, whereas H and Er decreased with increasing nanoindentation stress. Additionally, it has been noted that the H/Er and H_3/Er_2 ratios obtained through nanoindentation demonstrate a significant correlation between nanoindentation characterization and wear assessment obtained through conventional wear testing.

Balaji et al. (2015) studied the dry sliding pin-on-disc wear test behavior of Ti-(TiB/TiC) in situ composite by combining Ti-B_4C powder in three distinct quantities prepared through spark plasma sintering and reported that the evolution of the morphology and in situ phase creation improve the hardness and wear resistance of composite with increasing TiB and TiC particles also, improve titanium's wear resistance. The presence of Fe-rich wear debris acts as an in situ solid lubricant, reducing the average friction coefficient of the composites oxidation on the worn surface act as a protective layer to prevent further wear of the composite surfaces.

Choi et al. (2014) fabricated in situ (TiB+TiC) particulate-reinforced titanium matrix composites (TMCs)by vacuum induction melting and conducted a dry sliding ball on disk wear test with 52100 bearing steel ball of 6mm at fixed load set to 1, 3.5, and 10 N, sliding speed was 125 mm/s and duration was 30 min. It has been reported that 3.5 vol.% (TiB+TiC) composite at 10 N show less wear and coefficient of friction which is attributed to the oxide formation on debris, base material and reinforcement, a prominent wear mechanism was observed to be two-body abrasion.

Kim et al. (2011) synthesized titanium matrix composites (TMCs) with Conventional candidates for reinforcements like SiC, Si_3N_4, Al_2O_3, TiC, TiN, TiB, and TiB_2 using an investment casting process and reported that in situ synthesis method was also developed to ensure homogeneous distribution and a controlled interfacial reaction between the matrix and reinforcements. It has also been reported that the friction and wear behavior of TMCs using a pin-on-disk wear tester under various conditions and evaluated were using scanning electron microscopy (SEM) analysis.

Li et al. (2011) developed a titanium-based composite coating reinforced by in situ synthesized TiB whiskers and TiC particles was successfully fabricated on Ti6Al4V

by laser cladding. The coating is mainly composed of α-Ti cellular dendrites and a eutectic in which a large number of needle-shaped TiB whiskers and a few equiaxial TiC particles are uniformly embedded. The wear resistance of the coating is significantly superior to that of Ti6Al4V under the dry sliding wear condition at room temperature.

Lee et al. (2008) investigated the tribological performance of titanium alloy (Ti–6Al–4V) balls coated with a dual boride layer comprised of titanium diboride (TiB_2) and titanium boride (TiB) whiskers mated against alumina ceramic disks using lubricated ball-on-disk wear testing and reported that the wear rate of the boride-coated titanium alloy balls was found to be 40 times less than that of 97 percent dense alumina balls. It has been also reported that the enhanced wear resistance is due to the hardness and unique structure of the dual (TiB_2 + TiB) whisker layer and the resulting smoothness of the wear surface formed during the wear process. Compared to grain fracture and pullout in alumina, the material removal process in boride-coated balls is abrasive.

2.7 FORMULATION OF THE PROBLEM

A critical review of literature presented above suggests that despite a large number of investigations carried out to examine the microstructure and mechanical properties of Ti based composites containing various hard phases, only a few have been focused on synthesis of Ti-TiB composites containing relatively large volumes fraction of TiB. There is also a lack of studies on the evaluation of the friction and wear behavior of these type of composites, despite their ability to have excellent hardness and other mechanical properties. One may also infer from the above review of the literature that limited studies have been conducted on the evaluation of the tribological potential of Ti-TiB under reciprocating conditions at low to high frequencies. Therefore, it would be

proper to synthesize metal-based composites containing TiB as a reinforcing phase and analyze the effect of its content on the tribological behavior of prepared composites under dry sliding reciprocating condition.

In view of the above, the present study is being conducted to synthesize Ti-TiB composites containing different volume percentages of TiB via spark plasma sintering as well as vacuum arc melting. Two different sets of the composites are slated to be synthesized: (i) spark plasma sintered TiBFe composites containing a fixed amount of Boron and varying amount of Fe (10, 20 and 30 at. %) (TiBFe1010, TiBFe1020, TiBFe1030), and those containing a fixed amount of Fe with varying amount of Boron (10, 20 and 30 at. %) namely, TiBFe1010, TiBFe2010, TiBFe3010 and (ii) vacuum arc melted in-situ Ti-TiB composites having different content of TiB. The study also intends to evaluate the friction and wear characteristics these composites under different loads, frequencies by carrying out reciprocating wear tests at different loads and frequencies in order to elicit the effect of load, frequency and the volume percentage of TiB on their tribological performance apart from establishing the dominant wear of mechanisms.

2.8 OBJECTIVES OF STUDY

In light of the above, **the hypothesis is to develop Ti-TiB composites via Vaccum arc melting furnace and SPS. To find the optimized volume fraction by the tribological properties of the synthesized composite carrying a reciprocating test.** The present study has been carried out with the aim of fulfilling the following objectives:

i) To fabricate TiBFe composites containing a fixed amount of Boron and varying amount of Fe as well as composites containing a fixed amount of Fe with varying

amount of Boron (10, 20, and 30 at. %) via spark plasma sintering to explore the effect of B and Fe on the microstructure and hardness.

ii) To synthesize *in-situ* Ti-TiB composites containing different amount TiB via a cost effective vacuum arc melting route and to analyze the effect of the amount of TiB on microstructure and hardness of synthesized composites.

iii) To explore the friction and wear characteristics of the synthesized composites by carrying out reciprocating sliding wear tests at different loads and frequencies to elicit the influence of load, frequency and composition on their tribological performance and to determine the optimum TiB content for attaining optimum properties as well as optimum tribological performance.

iv) To establish the dominating mechanisms of wear.